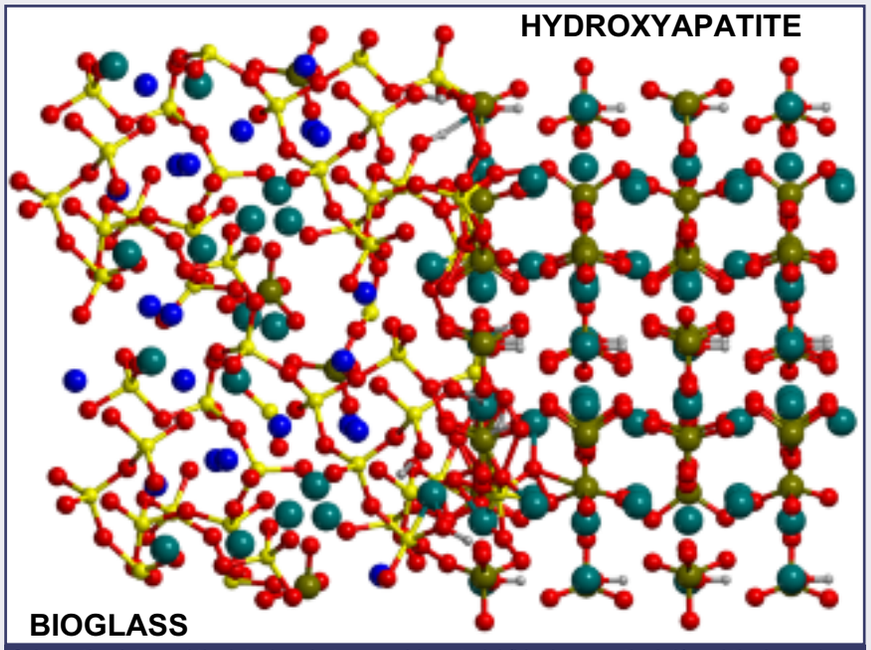

Schematic picture of the interface between a biomaterial (bioglass, on the left) and the bone, here represented by its mineral phase constituent (hydroxyapatite, on the right) when osteointegration occurs according to Hench mechanism

Alfonso Pedone[a,], Marta Corno[b]*
[a]Classe di Scienze
Scuola Normale Superiore di Pisa
[b]Dipartimento di Chimica IFM
NIS and INSTM
Università di Torino
alfonso.pedone@sns.it

COMPUTER SIMULATIONS TECHNIQUES FOR MODELLING BIOCERAMICS

Computational simulation of biomaterials constitutes a fundamental and fascinating research area, constantly growing thanks to the increasing availability of computational resources. The combined approach of classical and ab-initio methods has allowed the modelling of bioceramics (both bioactive glasses as the 45S5 Bioglass® and hydroxyapatite) and their complex interactions with the biological environment.

The simulation of matter at the atomic level by computer is now an essential tool of contemporary science. Atomic modelling techniques are used routinely in the study of proteins and pharmaceuticals and in the conformational analysis of organic molecules. Computational methodologies have, however, an equally important and diverse role in the study of inorganic materials, especially in complex systems such as microporous catalysts (zeolites and metal-organic frameworks, MOF), high temperature superconductors, ternary and quaternary oxides and biomaterials.

Nowadays, computational methods are routinely applied in several different fields: a) *modelling crystal structures*: such methods are used to assist the refinement of crystal structure data but the real challenge in this field is to develop procedures for predicting structures; b) there is perhaps an even greater incentive for the development of methods for *modelling amorphous structures* owing to the well-known difficulties in the determination of accurate and unambiguous atomistic structures for non-crystalline solids from experimental data alone; c) *modelling inorganic surface chemistry* is a field of growing importance and activity, since most of the reactivity of material with the surrounding environment occurs at their surfaces.

In this paper a review of recent progresses obtained in the field of computer simulations of biomaterials properties is provided. Far to be

exhaustive of the whole topic, this review will focus on the simulation of the structure, mechanical, dynamical properties of bioactive phospho-silicate glasses as well as surface reactivity of hydroxyapatite by means of classical and quantum-mechanical methods.
In the next section a brief introduction to bioceramics is offered, followed by general background of the computational methods available for crystalline and amorphous materials simulation.

Bioceramics: an open challenge

The huge technological advances in the development of orthopaedic and dental implants and bioceramic devices have considerably contributed to improve the quality of life over the last decades [1-4].
Bioceramics can be generally classified as bioinert (alumina and zirconia), resorbables (e.g. tricalcium phosphate) and bioactive (hydroxyapatite, bioactive glasses and glass-ceramics) on the basis of the response that the exposure of the implant elicits in the living environment.
After contact with biological fluids, inert biomaterials, such as titanium, stainless steel and cobalt alloys, are encapsulated within a non-adherent fibrous layer of variable thickness and the implant tissue interaction is essentially of mechanical nature. Interfacial movement under external stress leads to loosening and deterioration of the mechanical fit, which causes pain and eventually clinical failure of bioinert implants [5]. While porous ceramics can achieve a better mechanical fit thanks to tissue growth in the micropores [6], the absence of a real chemical adhesion with the tissues and the rigidity and fragility of ceramic materials still limit the long term durability of porous ceramic implants to generally less than 20 years (not adequate with the increasingly longer life expectancy). On the opposite extreme, "resorbable" or completely biodegradable materials, such as calcium phosphates, either crystalline or amorphous, are rapidly dissolved upon exposure to physiological fluids and gradually replaced by living tissues [7].
Among them, synthetic hydroxyapatite (HA) is employed in powder or porous form in the fields of bone tissue engineering, orthopaedic therapies [8] and as a coating of metallic prostheses. HA chemical and biological properties are strictly linked to its dimensions, which can be regulated with high biological and chemical control at the nano-scale. The use of nanotechnology is currently being explored to enhance the mechanical toughness of HA and to generate HA/biomolecules biomimetic matrices to improve the biological responses of HA. In fact, the surface functionalization of HA nano-crystals with bioactive molecules (phosphonates, bisphosphonates and amino acids) makes them able to transfer information to and to act selectively on the biological environment, and this represents a main challenge for innovative bone substitute materials. So, not only osteointegration or osteoinduction properties will be enhanced, but specific cellular responses will also be stimulated at the molecular level [9, 10].
Based on the natural ability of bone and muscles to self-heal and regenerate, the use of resorbable materials is in principle ideal, but the rates of implant dissolution and tissue growth have to be matched: while the implant is replaced by new tissue, its strength progressively decreases, leaving a very unstable interface that requires immobilisation of the patient for long periods.
The ideal compromise between inert and resorbable materials is represented by surface-active or bioactive materials. The first bioactive material, the melt-derived 45S5 Bioglass®, was discovered by Hench and coworkers in the 1970s [11]. These materials can be implanted and react chemically with body fluids [12], in aid of tissue reparation process by forming in the body a layer of biologically active bonelike carbonate-containing hydroxyapatite at the material surface. This layer then interacts with and incorporates biomolecules such as collagen, whereas further cellular steps lead to a strong and stable chemical bond between the glass and human hard (bone) and, in some cases, soft (muscles) tissues. The high effectiveness of the bioactive fixation process reflects the high strength of adhesion between the interface and both implant and tissues: in fact, the failure of bioactive implants in load bearing applications occurs in either the implant or the bone, but not at their interface. Failure in the implant reflects the weak mechanical strength (brittleness and limited fracture toughness) of bioactive glasses, whereas fracture in the bone is often related to stress shielding effects [1] because of the higher elastic modulus of the 45S5 Bioglass® compared to natural bone. The relatively poor mechanical properties limit clinical uses of melt-derived bioactive glasses to low-load bearing applications, such as otolaryngological, maxillofacial, dental and periodontal implants [4].
In the last years, much research has been focused on the addition of doping atoms in the original 45S5 Bioglass® to improve specific properties [13-15] for clinical applications. However, not all these efforts have always led to positive results, since some of the added oxides degraded or totally destroyed the bioactive behavior of the glasses.
Enhanced mechanical properties can be achieved by partial crystallization, as in the bioactive glass-ceramics where a tough ceramics phase reinforces the glass. For instance, A/W glass ceramics, composed of apatite and wollastonite crystals embedded in a calcium silicate amorphous phase, form a strong bond with bone but has also very good mechanical properties [3]. Therefore, they are successfully used in bone repair prostheses [16], even though the application to high load cases such as femoral and tibial bones are still not possible, and processing of glass ceramics biomaterials can be difficult and expensive.
Bioactive glasses can also be produced by the sol-gel synthesis route, first introduced in 1991 [17]. Sol-gel derived bioactive glasses showed an improved bioactivity compared to the melted ones, owing to their high porosity and high surface area [18], the latter known to enhance the superficial adhesion of biomolecules [19]. In the last years these favorable features have encouraged a significant shift in the research on bioactive silicate glasses towards highly porous materials. In particular, recent work has shown the high potential of bioactive glasses for 3rd-generation tissue-engineering applications [20], where a highly porous, biodegradable scaffold combined with tissue cells hosts the *in vitro* growth of immature bone like material, then implanted *in vivo* where the tissue-engineered construct adapts to the living environment and stable mature bone is formed [21].

Computational Techniques: *ab initio* vs classical methods

The growing technological importance of biomaterials has not been supported by a corresponding growth in fundamental understanding of the nature of their bioactivity, and trial-and-error approaches still represent the most common way to systematically optimize new applications of biomaterials. The availability of increasingly more powerful computational methods and resources now makes computer simulations an attractive alternative to experimental techniques, to obtain an atomistic view into the bioactive behaviour of such materials and to provide new insights into the structure-property relationships of materials.

At variance with crystalline materials, the computational modeling of amorphous solids is a difficult task, the immediate difficulty arising from the need to obtain atomistic models (coordinates of the atoms) that reproduce the known experimental features of the material. This is because no currently conceivable set of experiments leads to a unique structure of an amorphous compound and there is no rigorous definition of when it has been determined.

Molecular dynamics (MD) simulations may be considered the intuitive natural way to make a computer model of an amorphous or glassy material. In this framework, an equilibrated liquid is cooled through the glass transition to the final solid structure. Classical molecular dynamics (MD) simulations allow the study of structural, mechanical, thermodynamical and dynamical properties of relatively large systems (10^4-10^5 atoms) for long time scales (ns) [22-26]. However, the reliability of the obtained results strongly depends on the adequacy of the description of the interatomic potential, acting on the constituent ions. Parameters for amorphous materials are typically obtained from fitting to a set of experimental data measured on crystalline solids and therefore their domain of applicability has to be clearly understood and identified [23].

While standard force fields commonly used to model crystalline oxides are adequate to model pure and binary silicate glasses, their application to ternary and quaternary glasses is generally not as straightforward. This difficulty is mainly related to the mixed character of Si-O and P-O bonds, whose ionic-covalent balance depends on their local environment, such as the composition and geometry of the coordination shell of network-modifying cations in close proximity to the oxygen, and the bridging/non-bridging nature of the latter.

The effect of this diverse and often quite distorted local environment can hardly be reproduced by mean-field approaches using fixed partial charges and rigid-ion (RI) force fields. A practical and much more accurate way to take the molecular environment into account in classical MD simulations is via a shell-model (SM) approach, where the atomic polarizability is explicitly incorporated in the model by replacing polarizable atoms (typically the oxide ions for silicates) with core-shell dipoles consisting of two opposite charges connected by a harmonic spring [27, 28]. In this way, the charge distribution in silicate and phosphate groups is always consistent with the local electric field, and a better description of distorted bonded and non-bonded geometries, as well as of dynamical fluctuations at finite temperature, can be achieved.

A higher level of accuracy is achieved in *ab initio* simulations, where ionic forces are calculated using quantum mechanics methods: this parameter-free, first-principles approach clearly represents the best possible way to include polarization and other electronic effects in the MD model, making them extremely useful to tackle problems and systems which pose a serious challenge to empirical potentials, such as reactivity at surfaces or dynamical processes in melts.

A common approach in first-principles simulations of glasses is to obtain an initial structure through classical MD with an empirical potential and then switch to the *ab initio* treatment using the classical structure as 'starting guess' [29, 30].

However, this limits the scope of these mixed classical/*ab initio* approaches to investigate short-range features, or properties which turn out to have mainly local character (at least for these systems), such as the electronic structure and the vibrational spectrum [29-32].

Among the several *ab initio* codes applied in solid state modeling, there are two different classes: those employing plane waves and those adopting localized basis sets, as a linear combination of atom-centered Gaussian-type orbitals. Both choices have advantages and drawbacks, for instance plane waves basis set calculations with hybrid methods still is limited due to the delocalized nature of the basis functions while localized basis sets have to cope with the basis set superposition error which cause an overestimation of the interaction energy when dealing with adsorbate/surface interactions.

Bioceramics modelling

Silicate glasses are amorphous solids, characterized by a network of covalent SiO_4 tetrahedral building blocks, linked together by bridging oxygen (BO) atoms, each BO shared by two Si. While the short-range order within the tetrahedra is similar to their crystalline counterparts, no long range order is present; the high flexibility in the angle between linked tetrahedra and in their relative orientation determines a high degree of structural disorder beyond the short range.

Vitreous silica is characterized by a continuous network, fully interconnected in three dimensions, with every tetrahedron linked by BOs to four adjacent tetrahedra. The addition of alkali or alkaline-earth metal cations breaks the silicate network by replacing Si-BO-Si bonds with Si-NBO, where NBO is a non-bridging oxygen. They are thus called network modifiers in contrast to the silicon ions which are called network formers. According to the Modified Random Network (MRN) model [33] at high concentrations, the modifiers percolate through the bulk of the glass and form primary pathways, or channels, which play a key role in the elastic and transport properties of glasses.

The 45S5 Bioglass®: structure and dynamical properties

The microscopic structure of this material has been explored in higher detail by several classical molecular dynamics simulations employing both the rigid ionic model [29, 34] and the shell-model [35-37]. The coordination environment of network formers and modifiers [29, 38], the tendency to

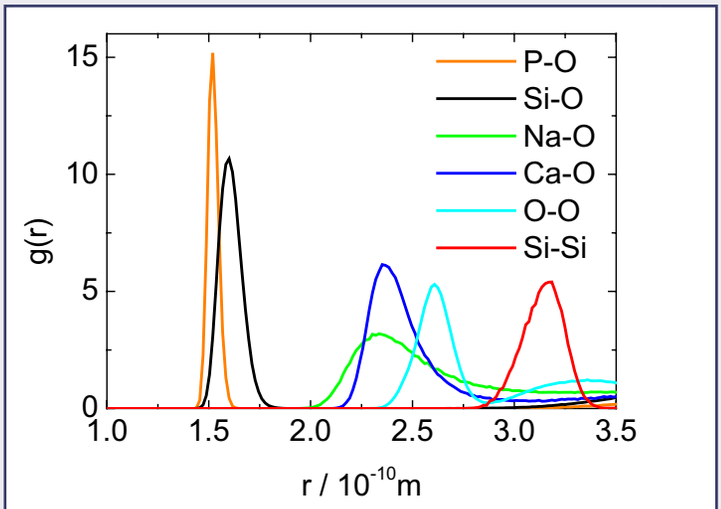

Fig. 1 - Radial distribution functions relative to the oxygen ion

form clusters and inhomogeneities [37, 39], the occurrence of chain and ring nanostructures [36] and the effect of phosphorous inclusion were discussed in relation to bioactivity [35] and medium-range order [34]. All these computational techniques showed to be in perfect agreement in reproducing short range geometrical features such as the coordination and bond distances of network formers and modifiers [29]. On the contrary, small differences were obtained in the structural parameters commonly used to describe the medium range order in amorphous glasses such as Q^n distributions (*n* is the number of bridging oxygens bounded to the network former cations Si or P). However, the trends in the distribution is captured by the rigid ionic model.

The environment around the cations present in the glass is analyzed through the pair distribution functions *g*(*r*) relative to the oxygen ions in Fig. 1. The structural features (bond lengths, coordination numbers and angles) have been calculated by using classical molecular dynamics simulations with the rigid ionic [29, 34] and shell-models [37] as well as by means of CPMD [38] simulations**.** All the models show that the intertetrahedal P-O distance of 1.52-1.55 Å is slightly shorter than the Si-O distance which is 1.59-1.63 Å, typical of silicate glasses. Moreover, P-NBO bonds are significantly shorter than Si-NBO bonds, and P-BO bonds are also shorter than Si-BO. These results show that the different strength of T-BO and T-NBO bond (T=Si/P) is well reproduced in our simulations.

The O-T-O bond angle distributions (BAD) reported in Fig. 2a is centred at the tetrahedral angle and show that O-P-O angle is more rigid than O-Si-O. The Na-O and Ca-O peak positions are between 2.33-2.34 and 2.29-2.35 Å, in the range of X-ray and neutron diffraction measurements for phosphate and soda-lime silicate glasses [40, 41], whereas the coordination shell of both Na and Ca is composed of about six oxygen atoms, whose arrangement is unveiled in the distribution of O-M-O angles in Fig. 2b.

Both distributions show a peak close to 90°, which generally results from Na or Ca atoms connecting two NBOs belonging to different tetrahedral, as shown in Fig. 3a. This result suggests an important structural role of modifier cations in controlling the folding of the silicate network by connecting and arranging together different chain-like and isolated fragments. The second peak at 60° (more pronounced for Na) results from modifiers coordinated to two NBOs (or one NBO and one BO) belonging to the same tetrahedron, as shown in Fig. 2b. The broad distributions of Fig. 2b also denote a high flexibility of the geometries of the coordination shell of these cations. Although the geometry of sodium and calcium coordination shells is qualitatively similar, the composition of these shells differs; there is a higher fraction of NBOs in the Ca coordination shell (5.4) with respect to Na coordination shell (4.4).

In 1992, Strnad introduced the concept of network connectivity (NC) [42], defined as the average number of BO atoms per glass-forming species (NC=4 for pure silica glass and NC=2 for chain-like structures), with the aim of predict and compare the bioactivity of different glass compositions. By comparing the NC of glasses with different bioactivity it was proposed a qualitative threshold of NC=3, that is glasses with NC<3 show bioactivity. A low NC denotes open and fragmented glass structures, whose rapid partial dissolution in aqueous physiological solution leads to HA formation and bone bonding in a short time. NC estimated from the glass composition is equal to 1.9 for the 45S5 Bioglass. NC can also be easily obtained by atomistic modelling, which enables the direct and unambiguous calculation of BOs per network-forming ion as well as the analysis of the network-forming role of different species [31].

In a recent work, Tilocca *et al.* [36] compared the MD structure of glass compositions of different (known) bioactive behaviours trying to identify correlations between medium range structural parameters (NC and Q^n speciation) and their bioactivities. They used three glass compositions

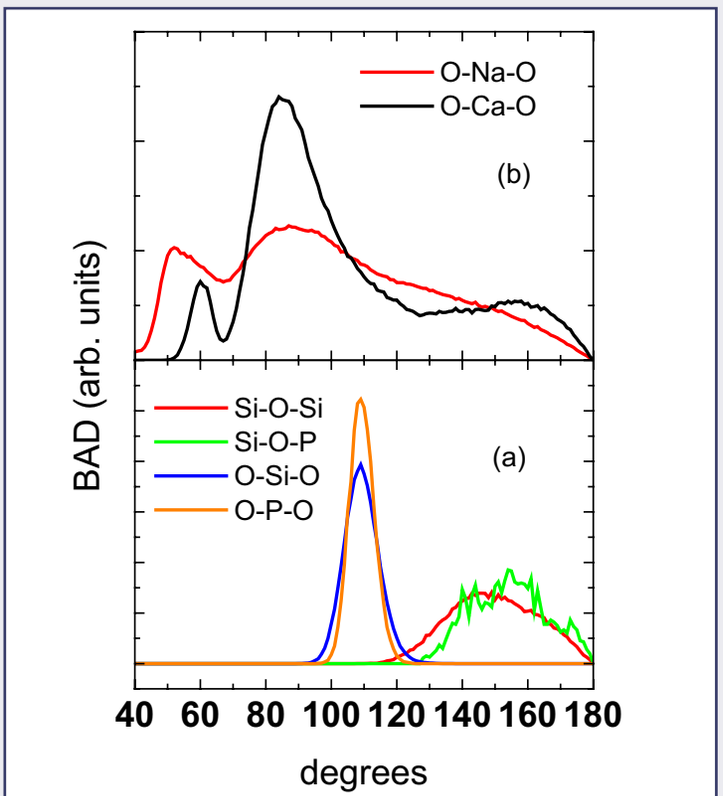

Fig. 2 - BAD functions: a) O-Si-O, O-P-O, Si-O-Si and Si-O-P and b) O-Na-O and O-Ca-O

ranging from very high (45S5), to intermediate (55S, 55% SiO_2) to bio-inactive (65S) and obtained NC of 2.07, 2.77 and 3.24 respectively. The Q^n(Si) distribution of 45S5 denotes that the highest bioactivity for this class of biomaterials arises from a structure dominated by chains of Q^2 metasilicates, which are occasionally cross-linked through Q^3 units, whereas the Q^1 species terminate the chains (Fig. 4). The comparison with the Q^n(Si) distribution of less bioactive compositions showed that the transition from high bioactivity (45S) to bio-inactivity (65S), through a region of intermediate bioactivity (55S), is accompanied by a shift of the Q^n distribution towards higher n values, with the 55S and 65S compositions dominated by Q^3 units.

It should be remarked that the current experimental picture of the Q^n speciation in 45S5 Bioglass is still somewhat incomplete; while a binary model with only Q^2 and Q^3 species is sometimes assumed [43], a three-component model with Q^1, Q^2 and Q^3 silicates was proposed to fit very recent nuclear magnetic resonance (NMR) data [34], and the presence of more than two Q^n(Si) species in this glass had already been inferred from previous Raman spectra [44]. Furthermore, given that the coexistence of several Q^n(Si) species in depolymerized alkali silicate glasses is well established [45], and that the presence of other species besides Q^1, Q^2 and Q^3 in 45S5 is less likely, the ternary Q^n(Si) distribution as in the recent models of 45S5, centred on Q^2, appears adequate [36, 46].

Concerning phosphate groups, it is normally assumed that they are predominantly isolated orthophosphates associated with modifier ions (Fig. 5), as proved by earlier investigations [43, 47, 48]. However, recent MAS-NMR experiments [34], IR and Raman data as well as computational simulations [32, 49-51] indicate that a small fraction of pyrophosphate (Q^1 or Si-O-P) species can coexist with the majority of orthophosphate species, which may affect the phosphate release rate due to the labile nature of surface P-O-Si bridges.

The molecular dynamics simulations using the rigid ionic model [34] yields a binomial distribution of Q^0 (about 60%) and Q^1 species while recent MD simulations with the shell-model potential improved the description of the phosphate speciation [50]. With the latter potential the fraction of orthophosphate units in 45S5 Bioglass is approximately 82%. It is worth to highlight that because of the low amount of P in the 45S5 Bioglass simulation boxes of about 10,000 atoms are necessary to reach converged Q^n(P) distributions.

The role of phosphorous on these glasses has been studied both experimentally and computationally. Several experimental works [52, 53] showed that certain phosphorous-free compositions can still be bioactive and apatite nucleation and crystallization can proceed by incorporating phosphate from physiological contact solutions. However, the incorporation of a small P_2O_5 fraction in the glass enhances the rate of HA deposition and bone-bonding ability [54]. Moreover, P-containing glasses promote the deposition of a more uniform HA film, which in turn, determines a stronger bond with bone.

This was interpreted by the low connectivity of phosphorous in the bioglasses which facilitates the release of phosphate species into the physiological fluid, this increases the local supersaturation and accelerates the HA

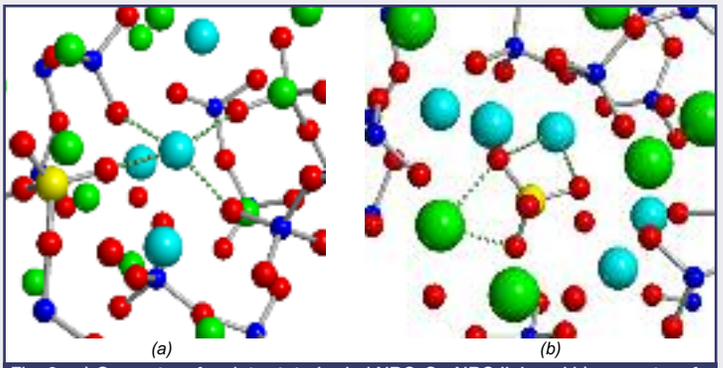

Fig. 3 - a) Geometry of an inter-tetrahedral NBO-Ca-NBO link and b) geometry of intra-tetrahedral NBO-Na-NBO and NBO-Ca-NBO. Silicon (blue) and oxygen (red) are represented as ball and sticks, whereas sodium (green) and calcium (cyan) are represented as spheres

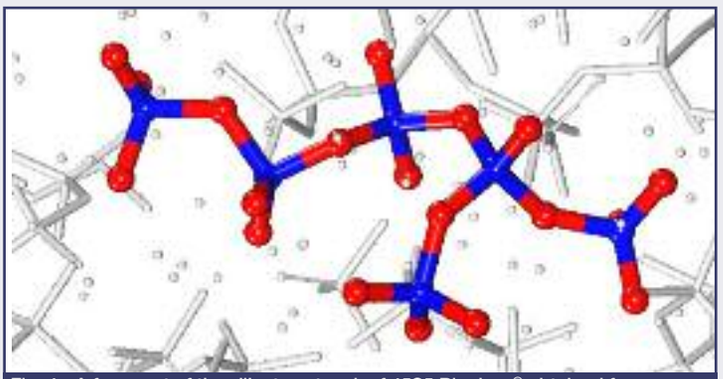

Fig. 4 - A fragment of the silicate network of 45S5 Bioglass® obtained from molecular dynamics simulations. Ball and stick visualization is used for the Si and O atoms of the fragment which are coloured in blue and red, respectively. The rest of the network is coloured in grey

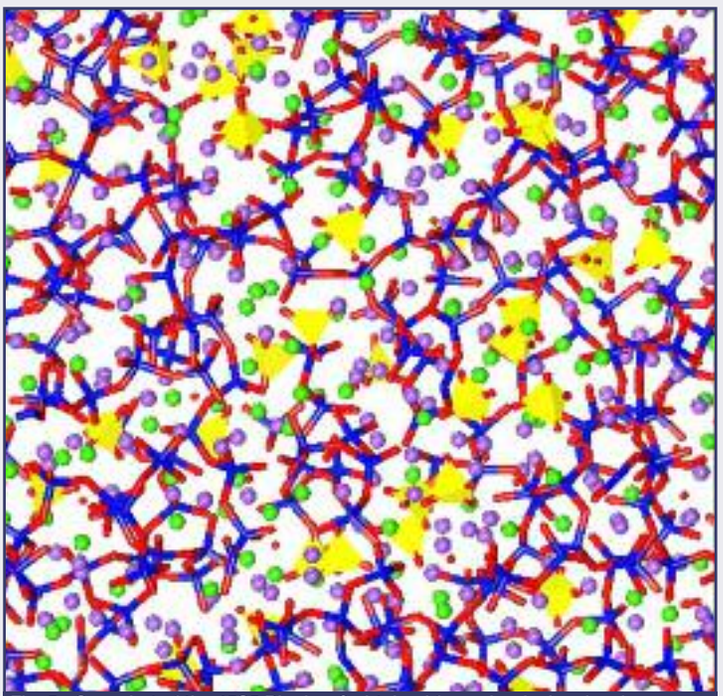

Fig. 5 - Snapshot of the 45S5 Bioglass® obtained from classical molecular dynamics simulations. Yellow tetrahedral represent orthophosphate units, blue and red sticks are Si and O atoms while green and cyan spheres are Ca and Na ions respectively

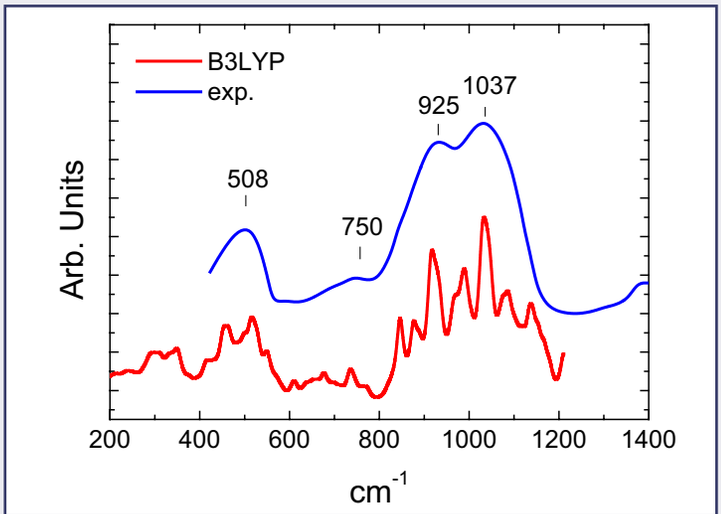

Fig. 6 - Experimental (blue line) and B3LYP (red line) IR spectra of the 45S5 Bioglass®

precipitation from the solution [53]. In a recent work, Malavasi *et al.* [55] tried to interpret the different bioactivity of CaO-SiO_2 and CaO-P_2O_5-SiO_2 glasses concluding that those compositions for which the orthophosphate units are surrounded by Ca ions with a ratio similar to that found in HA (that is 1.67) were the more bioactive.

Most of the previous works were devoted to the analysis of structural properties, while a detailed study of dynamical properties has not been addressed except for the calculation of the vibrational density of states by Fourier transforming of the velocity autocorrelation function calculated from CPMD trajectories [38, 49]. However, vibrational properties and the IR spectra of a complex material such as 45S5 glass can be simulated nowadays fully *ab initio* by means of modern quantum-mechanical codes like CRYSTAL06 [56].

This is a periodic *ab initio* program based on an atom centered (Gaussian) basis set which has allowed us to calculate the electronic properties and to simulate for the first time the IR spectra of the 45S5 Bioglass® [31, 32]. The calculated IR spectrum (broadened by Lorentzian functions with a typical width $\delta\nu$ = 40 cm^{-1}) is compared to the experimental one [15] in Fig. 6. Both the adsorption spectra show the same bands at 1,037, 925, 753, 600 and 500 cm^{-1}, being the experimental spectrum more broadened. From an experimentalist point of view, these wide bands are assigned as follows: the band at 1,037 cm^{-1} is associated to the asymmetric stretching of bridging oxygens (Si-BO-Si) in all Q species, the band at 925 cm^{-1} is assigned to the Si-NBO stretching vibrations in SiO_4 and it covers P-NBO stretching vibrations in PO_4 tetrahedra. The band around 600 cm^{-1} is assigned to the symmetric stretching vibrations of three membered siloxane rings of SiO_4 and to the O-P-O bending vibration in a PO_4 tetrahedra while the wide peak at 500 cm^{-1} is associated to O-Si-O bending vibrations in SiO_4 and symmetric oxygen stretching of Si-O-Si. A deep analysis of the vibrational features of such glass has been fully described in previous papers and it is out of the scope of this brief review.

At variance with our approach, Tilocca *et al.* [38] assigned specific vibrational features in the overall vibrational spectrum of the 45S5 glass by calculating the vibrational (power) spectrum obtained from a Car-Parrinello MD trajectory. The excellent agreement found with the phonon frequencies computed by us from the eigenvalues of the Hessian matrix in the harmonic approximation shows that anharmonic effects (included in the CPMD power spectrum) are small for this system [32].

Among the computational studies found in literature, few works have been devoted to the simulation of the effect of doping ions on the structure of bioactive glasses [14, 57] and despite the paramount importance of transport, elastic and mechanical properties no such simulations have been carried out so far.

A first attempt was carried out by Pedone *et al.* [46] who studied the effect of the replacement of CaO for MgO on the structural properties of the 45S5 Bioglass®. The results confirmed the complexity of the local environment of Mg ions which are coordinated predominantly by 5 non-bridging oxygens of different TO_4 tetrahedra (T=Si/P) leading to large rings in the structures. A rough correlation between the average dimension of the rings found in the structure and the computed Young's modulus was obtained. The Young's modulus decrease at low Mg-content reaching a minimum for the $46.2SiO_2{\cdot}24.3Na_2O{\cdot}16.9CaO{\cdot}2.6P_2O_5{\cdot}10MgO$ glass. Mg was found to be homogeneously distributed in the silica rich region together with Ca and Na ions but was almost totally absent from the Ca-Na-phosphate rich regions. A systematic analysis of the structural changes induced by replacing SiO_2 by P_2O_5 in bioactive compositions has highlighted that increasing the P_2O_5 fraction leads to repolymerization of the silicate network. This was interpreted on the basis of the higher affinity of Na and Ca cations for phosphate groups, which are able to strip the modifier cations out of the silicate network, thus inducing its repolymerization [35].

Lusvardi *et al.* [14, 57] performed molecular dynamics simulation study of the nanosegregation promoted by the incorporation of fluorine ions in bioactive glasses. The results showed that the high affinity of fluorine for Na and Ca modifier cations determines the separation of a highly polymerized phosphosilicate matrix from an ionic phase rich in Na, Ca and F. Conversely, fluorine-free bioglasses favour the separation of a phosphate-rich phase from a silica-rich one [37, 39].

Hydroxyapatite: bulk properties and surface reactivity

Hydroxyapatite is a calcium phosphate mineral and belongs to the crystal family of calcium apatites (HA, $[Ca_{10}(PO_4)_6X_2]$, with X = OH^-, Cl^-, F^- or Br^-). Generally, calcium can be partially or completely substituted with Pb^{2+}, Sr^{2+}, Na^+, Mg^{2+}, K^+, Li^+, Fe^{2+}, Mn^{2+}, Zn^{2+} and Cu^{2+}. Among the commonly substituted ions into the hydroxyapatite lattice there are also carbonates, for whose two different substitutions are proposed: $OH^{\bullet}$ (type A) or PO_4^{3-} (type B). Type A usually occurs in high-temperature apatites, while type B in low-temperature materials [58, 59]. In nature, stoichiometric hydroxyapatite is found in the monoclinic form ($P2_1/b$ space group), while the non stoichiometric and most frequently encountered HA is within the hexagonal form ($P6_3/m$ space group). The main difference in crystal structures is the alignment of hydroxyl groups with respect to the *c* lattice vector, since the hexagonal phase is affected by protonic disorder, while in the monoclinic

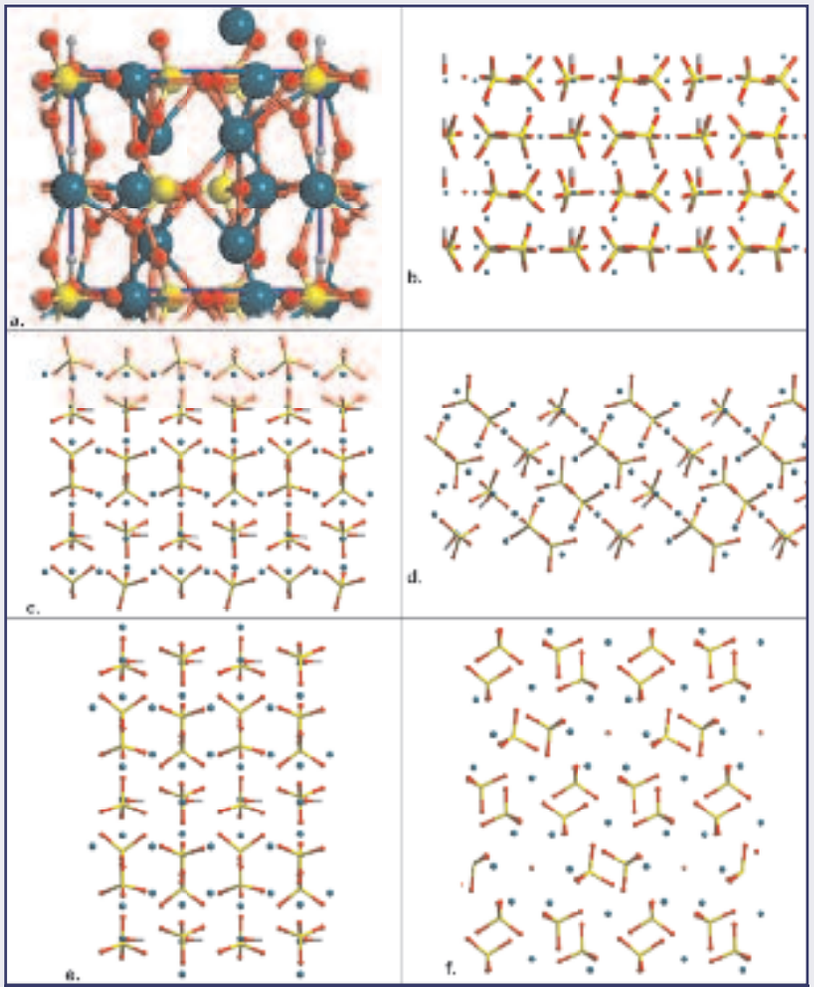

Fig. 7 - Hexagonal hydroxyapatite bulk and surfaces as modeled by the slab model approach and optimised by CRYSTAL06 code a) bulk; b) (001); c) (010); d) (101); e) non stoichiometric (010) calcium rich; f) non stoichiometric (010) phosphorus rich. Color coding: calcium ions in cyan, oxygen red, phosphorus yellow and hydrogen light grey

case OH groups are oriented upward and downward in alternating columns. The phase transition between the monoclinic and the hexagonal forms occurs at temperatures above about 200 °C, so that the monoclinic HA is considered a low-temperature structure [60]. The transition is also called an order/disorder transition, since the highly ordered columns of hydroxyl groups present in the monoclinic phase turn to protonic disorder of the hexagonal form, as it has been simulated by means of Molecular Dynamics by Zahn and co-workers [61].

The computational study of the hydroxyapatite material ideally starts from this point, *i.e.* the bulk structure in one of its form, monoclinic or hexagonal. Nevertheless, when applying quantum-mechanical methods, there are two problems: i) the higher computational cost of the monoclinic structure with respect to the hexagonal one (88 atoms compared to 44 in the unit cell, respectively) and ii) the proton disorder of the hexagonal structure as determined by X-ray diffraction [62, 63]. So, to overcome both problems, a strategy can be that of considering hexagonal hydroxyapatite and lowering the symmetry from $P6_3/m$ to $P6_3$, thus eliminating the mirror plane *m*, responsible of replicating H atoms in non chemically sensible positions [64]. The result is a hexagonal HA with hydroxyl groups all aligned upwards with respect to the positive directions of *c* lattice vector, in a doable 44 atoms unit cell. The presence of this OH alignment does not destabilize the bulk structure, since the unit cell is repeated to the infinite in the three dimension by translational operators. The obtained hexagonal HA bulk structure has then been fully optimized (internal coordinates and lattice parameters, see Fig. 7a) to find the minimum energy geometry with different functionals and basis set (among the others: B3LYP DPZ Gaussian [64], LDA Perdew-Zunger numerical DZP [65], GGA PW91 plane waves ultra-soft pseudopotential E_{cut}=500 eV [66]).

An interesting result of the simulation is the computed vibrational spectrum of the material, that can be compared to experimental data to help in the often complex band assignment and interpretation. By means of the CRYSTAL code, the complete IR spectrum has been simulated at Γ point (IR and Raman spectra refer to that point) within the harmonic approximation and the comparison with experimental data is very satisfying [64]. This work goes beyond the limits of *ab initio* calculations pointed out by Calderìn and co-authors, who reported a shell model study of lattice dynamic of hydroxyapatite [67].

More challenging is surface modeling starting from an optimized bulk structure of the material. Surfaces are the real place where reactions occur, especially for biomaterials in continuous contact with biological fluids. When simulating a surface, the first question is: which one? Since infinite surfaces can be extracted from the bulk, a preliminary study of crystal forms is mandatory as well as a literature research to see whether other studies regard one particular face.

Regarding how to model a surface, different possible models exist. In plane waves based codes, it is very common to design a system repeated infinitely in the three dimensions, with the one corresponding to the chosen face separated from the other replica by vacuum, *i.e.* a not really 2D slab. The main alternative is the so called “slab model”, where the surface is terminated with two faces and characterized by a finite thickness as a real bi-dimensional system. This approach is used when the basis set is localized functions, as Gaussian ones and here we describe it in details, referring to recent work done on HA [68]. In practice, when defining the slab, one chooses how many atomic layers will be contained inside the unit cell, being this layers classified in terms of their *z* coordinate. When possible it is better to maintain the symmetry along the structure cutting two symmetric layers as the top and the bottom faces. Sometimes it is necessary to add atoms at dangling bonds, chemically reconstructing the surface. It is well known by literature that the most common faces of hexagonal hydroxyapatite are the (001) and the (010), which is equivalent to the (100) in the hexagonal lattice. The (001) surface is involved in bone and enamel growth, while the (010) is very extended in the crystal and is proved to strongly interact with different biomolecules [69, 70]. Since the starting model is the bulk with $P6_3$ symmetry, the corresponding (001) surface has a *P3* symmetry and it represents a quite complex case to study due to fer-

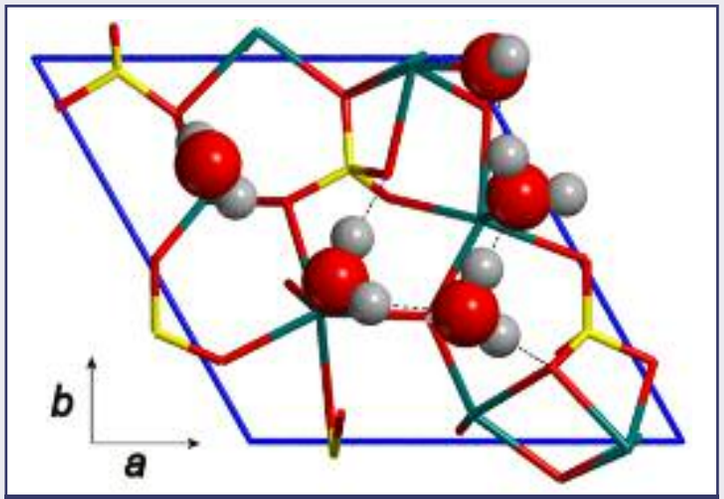

Fig. 8 - Water on hexagonal HA (001) surface: maximum loading model, as seen from above, to highlight the cooperation of hydrogen bonding at surface. Water atoms displayed with van der Waals spheres, while surface atoms with sticks. Color coding: calcium ions in cyan, oxygen red, phosphorus yellow and hydrogen light grey

roelectric behavior imposed by OHs alignment along the finite direction of the slab (see Fig. 7b). No details are given here and an interested reader could shift to references [68] and [71] for a deep discussion, referring also to a recently developed shell-ion model potential for HA [28], concluding that a slab thickness of about 14 Å is a good model for (001) surfaces.

On the other hand, the (010) surface does not show any symmetry operator and OH groups lay parallel to the *ab* plane, not influencing stability (see Fig. 7c) [51].

Going further with most stable HA stoichiometric surfaces, also the (101) face, equivalent to the (110) one, has been modeled (see Fig. 7d), which shows a diagonal alignment of OH groups. The stability order of these three structures in terms of their surface energy is (001)>(101)>(010) - 1.043, 1.646 and 1.709 Jm^{-2} [71], respectively - in agreement with other computational studies [72-74].

To complete the description, according to a recent HRTEM study by Sato *et al.* [75], non-stoichiometric surfaces of (010) termination can play a role. Following the approach adopted by Astala and Stott [72], two non-stoichiometric (010) surfaces were designed: a calcium rich model (Ca/P: 1.71, Fig. 7e) and a phosphorus rich one (Ca/P=1.62, Fig. 7f). The modeling procedure is based on the classification of two electroneutral layers along the (010) termination, called A-type ($Ca_3(PO_4)_2$) and B-type ($Ca_4(PO_4)_2(OH)_2$). Being A-B-A-A-B-A the stoichiometric termination, the other alternatives generate the Ca-rich and P-rich surfaces, the first revealing a higher nucleophylic character by the electrostatic potential maps analysis (not shown for brevity, refer to [71]).

Each surface model is then fully characterized to investigate its adsorptive features, particularly by means of electrostatic potential mapping at almost 2 Å above and below the two external faces. Irrespective of the considered slab, all models show strongly positive potential in correspondence to more exposed calcium ions and negative values associated to phosphate groups. The co-presence of these two aspects guides the interactions with polar biomolecules, such as water and amino acids.

To exhaustively review all the computational studies on hydroxyapatite surfaces in interaction with different molecules goes beyond the scope of this work. In the following, some recent results will be synthetically reported about HA surfaces in interaction with water and glycine, to give a taste of what it can be done nowadays with the simulation of biomaterials interfaces with biomolecules.

Water represents a fundamental molecule in the biological environment, so that a deep understanding of its role in HA surface adsorption processes - both alone and in association with other biomolecule - is the first step to investigate. In a recent *ab initio* based computational work, Corno *et al.* have simulated water adsorption on the hexagonal (001) and (010) faces previously described (Fig. 7b,c) to investigate if the interaction was molecular or dissociative [51]. At first, one water per each exposed calcium ion of both upper and lower faces of the two slabs was adsorbed, so to compare interaction energies on different reaction sites. Then higher water loading on the same face has been modeled and interaction energies compared to microcalorimetric heats of adsorption, showing a good agreement. The results are quite different according to the specific slab, that is on (001) slab there is always molecular adsorption (ΔE=-100 $kJmol^{-1}$ per adsorbed water molecule), while for (010) mainly dissociative adsorption is observed (highly energetic, ΔE~-300 $kJmol^{-1}$), with the formation of new surface functionalities (CaOH and POH). The (010) surface after reaction with water was called (010)_R and fully relaxed to be used as a new model for further water loading, showing molecular adsorption with energies comparable to those of the (001) case. The computed IR spectra of adsorbed water showed very strong red shifts of the OH stretching frequencies, due to the formation of superficial hydrogen bonds between water hydrogen and phosphate groups oxygen, in line with experimental results [51]. Fig. 8 shows the maximum loading model of (001) surface as seen in a top view. This study has been then further extended to deal with the other modeled surfaces, *i.e.* (101) and (010) non-stoichiometric ones, showing similar results not described for brevity [71].

In the literature, Zahn *et al.* have studied the interfaces between hydroxyapatite and H_2O by means of molecular dynamics simulation, hydrating different types of the (001) and (00-1) surfaces of monoclinic hydroxyapatite (obtained as slices of a block of 3x3x3 unit cells) by a large number of H_2O molecules. They observed several strongly ordered hydration layers, the first of which characterized by a network of strong electrostatic/hydrogen bonds reducing H_2O mobility [76].

Applying molecular dynamics techniques, also Pan *et al.* have studied the H_2O behaviour on hydroxyapatite (100) and (001) crystal faces, considering about 1,550 molecules on both surfaces and described the formation of three highly structured H_2O layers on both faces [77].

As for other recent *ab initio* density functional studies, Ma and Ellis have simulated the initial stages of the hydration process (PW91 functional and plane waves basis set) [78], while in the already mentioned work of Astala and Stott the SIESTA code (PBE functional) has been applied to study hydration of (001), (010), (101) and non-stoichiometric surfaces [72].

The abovementioned theoretical works on hydration of HA surfaces represent only a small part of the large number of papers dealing with this mate-

rial in interaction with inorganic and organic molecules (citric acid [73, 79] and biphosphonates [80], just to cite two interesting cases). The next step in these study is to increase the adsorbate complexity, for instance considering the fundamental molecules in the biological environment, *i.e.* amino acids. On both (001) and (100) surfaces of HA Pan *et al.* simulated the adsorption of the amino acids glycine and glutamic acid by means of MD simulations [81]. Huq *et al.* investigated the interaction of the motif Ser(*P*)-Ser(*P*)-Ser(*P*)-Glu-Glu with monoclinic HA (001), (010) and (100) surfaces (the last two slabs generated with different cleavage planes) and it resulted that the motif had preference for (100) and (010) faces, due to electrostatic interactions between acidic site groups and surface calcium ions [82].

As for *ab initio* calculations, following the same procedure adopted for water adsorption, Rimola *et al.* have studied glycine adsorption on (001) and (010)_R HA surfaces, showing that on the first surface glycine adsorbs in its zwitterionic form, while on the latter an ionic pair is formed, due to a spontaneous proton transfer towards the surface [83]. Since the simulation has regarded adsorption at the gas-phase, the next logic question has dealt with the role of water in the process, that is investigating the competitive adsorption between glycine and water. A recent approach to the problem has been proposed by the same authors of the previous paper and it is based on a series of static calculations of progressive micro-solvation of the dry interface of glycine adsorbed on the (001) surface of hydroxyapatite [84]. Despite all the methodology limitations, the conclusion is that glycine directly adsorbs on HA surfaces, or via one water molecule maximum, due to the strong affinity of the amino acid to the inorganic surface. Interestingly, recent experimental results of grazing incidence X-ray diffraction measurements on the aqueous Gly-fluoroapatite surface have shown the direct contact of glycine and the surface [85], so confirming computational findings and suggesting to go further with the computational study, increasing once more the system complexity.

Conclusions

Computational techniques have been shown to be capable of help in the fundamental knowledge of complex problems in the field of biomaterial research. Among the large number of biomaterials, both 45S5 Bioglass® and hydroxyapatite have been the object of several experimental studies, though the understanding at a molecular level of the integration mechanism in bones and teeth has not been fully reached yet. To this target, computational modelling represents a crucial tool to complement and interpret experimental data. Applying different methodologies, from classical dynamics to *ab initio*, bulk properties of amorphous materials as well as surface reactivity of crystalline structures can be characterised. In the present work, two examples of biomaterial modelling have been described: structural and dynamical properties of 45S5 Bioglass® and surface characterisation and reactivity of hydroxyapatite. Nice agreement with experimental results have validated both models, suggesting to go further. Much investigation has still to be carried on, as the complex mechanisms of the human body do constitute an open challenge, and the synergic interplay of experimental and computational simulations has become essential.

Acknowledgments: The authors would like to acknowledge collaboration and interaction with Professor M.C. Menziani, Prof. L. Menabue, Dr. G. Malavasi, and G. Lusvardi (Università di Modena e Reggio Emilia, Italy), Prof. P. Ugliengo (Università di Torino, Italy), Dr. A. Rimola (Universitat Autònoma de Barcelona, Spain), Prof. V. Bolis (Università del Piemonte Orientale, Italy), Professor A.N. Cormack (Alfred University, USA) and Dr. Antonio Tilocca (University College of London, UK). DEISA Extreme Computing Initiative (BIOGLASS Project) is gratefully acknowledged for allowance of computer resources. M. C. acknowledges financial support by the Italian Ministry MIUR (Project COFIN-2006, Prot. 2006032335 Interface phenomena in silica-based nanostructured biocompatible materials contacted with biological systems).

Alfonso Pedone was born in Atripalda (AV), June 26, 1980. He received his degree and Ph.D in chemistry at the Università di Modena e Reggio Emilia. Currently, he has a post-doc position at Scuola Normale Superiore of Pisa. He performs research activity in the field of computer simulations based on QM/MM methods applied to the study of biomaterials, nitroxide spin probes and organic dyes. He spent periods of study in Italian and foreign research institutes; in particular, he has been a visiting scientist at the Università di Torino, Alfred University, NY (USA), and Università di Napoli. He has been awarded with the Modena Rotary Club prize titled "The best scientific brains" and the "Primo Levi Prize 2006" for the best young Italian researcher in chemistry released by the Italian Chemical Society. He took part to several congresses and workshops as speaker and he is coauthor of about 30 articles published on international scientific journals.

Marta Corno was born in Turin on February 25, 1981. She received her degree and Ph.D in chemistry at the Università di Torino. At present she is a post-doctoral Research Fellow at the Department of Chemistry IFM in Turin. Her research interests have concerned the study of biomaterials, such as hydroxyapatite and bioactive glasses by means of high-level periodic quantum mechanical calculations with the CRYSTAL code. Recently, she has started working on ab initio calculations on hydrogen storage materials, such as light metal hydrides (European FP7 Project FLYHY).

References

[1] L.L. Hench, *J. Am. Ceram. Soc.*, 1998, **81**, 1705.
[2] M. Vallet-Regi, *J. Chem. Soc., Dalton Trans.*, 2001, 97.
[3] T. Kokubo *et al., Biomaterials*, 2003, **24**, 2161.
[4] M. Cerruti, N. Sahai, *Rev. Min. Geochem.*, 2006, **64**, 283.
[5] L.L. Hench, *Biomaterials*, 1998, **19**, 1419.
[6] S.F. Hulbert, The use of Alumina and Zirconia in surgical implants, World Scientific, London, U.K., 1993.
[7] J.C. Knowles, *J. Mater. Chem.*, 2003, **13**, 2395.
[8] N. Roveri, B. Palazzo, Tissue, Cell and Organ Engineering, Wiley-VCH, Weinheim, 2006.
[9] B. Palazzo *et al., Adv. Funct. Mater.*, 2007, **17**, 2180.
[10] B. Palazzo *et al., Acta Biomaterialia*, 2009, **5**, 1241.
[11] L.L. Hench *et al., J. Biomed. Mater. Res.*, 1971, **2**, 117.
[12] T. Kokubo *et al., J. Biomed. Mater. Res. Symp.*, 1990, **24**, 721.
[13] O.H. Andersson *et al., J. Non. Cryst. Solids*, 1990, **119**, 290.
[14] G. Lusvardi *et al., J. Phys. Chem. B*, 2008, **112**, 12730.
[15] G. Lusvardi *et al., J. Biomater. Appl.*, 2008, **22**, 505.
[16] T. Yamamuro, A/W glass-ceramic: clinical applications, World Scientific, Singapore, 1993.
[17] R. Li *et al., J. Appl. Biomater.*, 1991, **2**, 231.
[18] M.M. Pereira *et al., J. Am. Ceram. Soc.*, 1995, **78**, 2463.
[19] S. Levy *et al., J. Mater. Sci.; Mater. Med.*, 2007, **18**, 89.
[20] L.L. Hench, J. M. Polak, *Science*, 2002, **295**, 1014.
[21] J.R. Jones *et al., Biomaterials*, 2007, **28**, 1653.
[22] A. Pedone, *J. Phys. Chem. C*, 2009, **113**, 20773.
[23] A. Pedone *et al., J. Phys. Chem. B*, 2006, **110**, 11780.
[24] A. Pedone *et al., Chem. Mater.*, 2007, **19(13)**, 3144.
[25] A. Pedone *et al., Theor. Chem. Acc.*, 2008, **120**, 557.
[26] A. Pedone *et al., J. Phys. Chem. C*, 2008, **112**, 11034.
[27] A. Pedone *et al., Chem. Mater.*, 2008, **20**, 2522.
[28] A. Pedone *et al., J. Mater. Chem.*, 2007, **17**, 2061.
[29] G. Malavasi *et al., Theor. Chem. Acc.*, 2007, **117**, 933.
[30] A. Tilocca, N.H. de Leeuw, *J. Mater. Chem.*, 2006, **16**, 1950.
[31] M. Corno, A. Pedone, *Chem. Phys. Lett.*, 2009, **476**, 218.
[32] M. Corno *et al., Chem Mater.*, 2008, **20**, 56105621.
[33] G.N. Greaves, *Phil. Mag. B*, 1989, **60**, 793.
[34] L. Linati *et al., J. Non-Cryst. Solids*, 2008, **354**, 84.
[35] A. Tilocca, A.N. Cormack, *J. Phys. Chem. B*, 2007, **111**, 14256.
[36] A. Tilocca *et al., Faraday Discuss.*, 2007, **136**, 45.
[37] A. Tilocca *et al., Chem. Mater.*, 2007, **19**, 95.
[38] A. Tilocca, N.H. de Leeuw, *J. Phys. Chem. B*, 2006, **110**, 51.
[39] G. Lusvardi *et al., J. Phys. Chem. B*, 2005, **109**, 21586.
[40] R.K. Brow, *J. Non-Cryst. Solids*, 2000, **263-264**, 1.
[41] M. Dubiel *et al., J. Non-Cryst. Solids*, 1997, **220**, 30.
[42] Z. Strnad, *Biomaterials*, 1992, **13**, 317.
[43] V. FitzGerald *et al., Adv. Func. Mater.*, 2007, **17**, 3746.
[44] C.C. Lin *et al., J. Non-Cryst. Solids*, 2005, **351**, 3195.
[45] H. Maekawa *et al., J. Non-Cryst. Solids*, 1991, **127**, 53.
[46] A. Pedone *et al., J. Phys. Chem. C* 2009, **113**, 15723.
[47] I. Elgayar *et al., J. Non-Cryst. Solids*, 2005, **351**, 173.
[48] M.W.G. Lockyer *et al., J. Non-Cryst. Solids*, 1995, **188**, 207.
[49] A. Tilocca, *Phys. Rev. B*, 2007, **76**, 224202.
[50] A. Tilocca, *J. Chem. Phys.*, 2008, **129**, 084504.
[51] M. Corno *et al., Langmuir*, 2009, **25**, 2188.
[52] Y. Ebisawa *et al., Biomaterials*, 1997, **18**, 1277.
[53] O.H. Andersson, *J. Mater. Sci.: Mater. Med.*, 1992, **3**, 326.
[54] M. Vallet-Regì *et al., Chem. Mater.*, 2005, **17**, 1874.
[55] G. Malavasi *et al., submitted to J. Phys. Chem. C.*
[56] R. Dovesi *et al.,* CRYSTAL2006 User's Manual, 2006, Università di Torino (Italy).
[57] G. Lusvardi *et al., J. Phys. Chem. B*, 2002, **106**, 9753.
[58] R. Astala, M. Stott, *J. Chem. Mat.*, 2005, **17**, 4125.
[59] J.A.L. Rabone, N.H. de Leeuw, *Phys. Chem. Miner.*, 2007, **34**, 495.
[60] H. Suda *et al., J. Phys. Chem.* , 1995, **99**, 6752.
[61] O. Hochrein *et al., Chem. Mater.*, 2005, **17**, 1978.
[62] J.M. Hughes *et al., Am. Mineral.*, 1989, **74**, 870.
[63] A.T. Saenger, W.F. Kuhs, *Z. Kristallogr.*, 1992, **199**, 123.
[64] M. Corno *et al., Phys. Chem. Chem. Phys.*, 2006, **8**, 2464.
[65] L. Calderin *et al., Phys. Rev. B*, 2003, **67**, 134106.
[66] D. Haverty *et al., Phys. Rev. B*, 2005, **71**, 094103.
[67] L. Calderin *et al., Phys. Rev. B* 2005, **72**, 224304.
[68] M. Corno *et al., Eur. J. Mineral.*, 2007, **19**, 757.
[69] J. Kirkham *et al., Curr. Opin. Colloid Interface Sci.*, 2002, **7**, 124.
[70] J.P. Simmer, A.G. Fincham, *Crit. Rev. Oral Biol. Med.*, 1995, **6**, 84.
[71] M. Corno *et al., Phys. Chem. Chem. Phys.*, 2010, **12**, 6309.
[72] R. Astala, M.J. Stott, *Phys. Rev. B*, 2008, **78**, 075427.
[73] M.R.T. Filgueiras *et al., J. Cryst. Growth*, 2006, **294**, 60.
[74] P. Rulis *et al., Phys. Rev. B*, 2007, **76**, 245410.
[75] K. Sato *et al., J. Am. Ceram. Soc.*, 2002, **85**, 3054.
[76] D. Zahn, O. Hochrein, *Phys. Chem. Chem. Phys.*, 2003, **5**, 4004.
[77] H. Pan *et al., Front. Chem. China* 2007, **2**, 156.
[78] X. Ma, D.E. Ellis, *Biomaterials*, 2008, **29**, 257.
[79] N.H. de Leeuw, J.A.L. Rabone, *Crystengcomm* 2007, **9**, 1178.
[80] J. Robinson *et al., J. Mol. Struct.*, 2006, **825**, 134.
[81] H. Pan *et al., Langmuir* 2007, **23**, 8972.
[82] N.L. Huq *et al., J. Mol. Model.* , 2000, **6**, 35.
[83] A. Rimola *et al., J. Am. Chem. Soc.*, 2008, **130**, 16181.
[84] A. Rimola *et al., Phys. Chem. Chem. Phys.*, 2009, **11**, 9005.
[85] A. Pareek *et al., Langmuir*, 2009, **25**, 1453.

RIASSUNTO

Simulazione computazionale per la modellazione di materiali bioceramici

La simulazione computazionale di biomateriali costituisce un fondamentale e affascinante ambito di ricerca, in costante sviluppo grazie alla crescente disponibilità di risorse di calcolo. L'uso combinato di tecniche classiche e metodi ab-initio ha permesso la modellizzazione di materiali bioceramici (sia vetri bioattivi, come il biovetro 45S5®, sia idrossiapatite) e delle loro complesse interazioni con l'ambiente biologico.